

A Fully General, Non-Perturbative Treatment of Impulsive Heating

Uddipan Banik^{1*}, Frank C. van den Bosch¹

¹*Department of Astronomy, Yale University, P.O. Box 208101, New Haven, CT 06520, USA*

ABSTRACT

Impulsive encounters between astrophysical objects are usually treated using the distant tide approximation (DTA) for which the impact parameter, b , is assumed to be significantly larger than the characteristic radii of the subject, r_S , and the perturber, r_P . The perturber potential is then expanded as a multipole series and truncated at the quadrupole term. When the perturber is more extended than the subject, this standard approach can be extended to the case where $r_S \ll b < r_P$. However, for encounters with b of order r_S or smaller, the DTA typically overpredicts the impulse, $\Delta \mathbf{v}$, and hence the internal energy change of the subject, ΔE_{int} . This is unfortunate, as these close encounters are, from an astrophysical point of view, the most interesting, potentially leading to tidal capture, mass stripping, or tidal disruption. Another drawback of the DTA is that ΔE_{int} is proportional to the moment of inertia, which diverges unless the subject is truncated or has a density profile that falls off faster than r^{-5} . To overcome these shortcomings, this paper presents a fully general, non-perturbative treatment of impulsive encounters which is valid for any impact parameter, and not hampered by divergence issues, thereby negating the necessity to truncate the subject. We present analytical expressions for $\Delta \mathbf{v}$ for a variety of perturber profiles, and apply our formalism to both straight-path encounters and eccentric orbits.

Key words: methods: analytical — gravitation — galaxies: interactions — galaxies: kinematics and dynamics — galaxies: star clusters: general — galaxies: haloes

1 INTRODUCTION

When an extended object, hereafter the subject, has a gravitational encounter with another massive body, hereafter the perturber, it induces a tidal distortion that causes a transfer of orbital energy to internal energy of the body (i.e., coherent bulk motion is transferred into random motion). Gravitational encounters therefore are a means by which two unbound objects can become bound (‘tidal capture’), and ultimately merge. They also cause a heating and deformation of the subject, which can result in mass loss and even a complete disruption of the subject. Gravitational encounters thus play an important role in many areas of astrophysics, including, among others, the merging of galaxies and dark matter halos (e.g., [Richstone 1975, 1976](#); [White 1978](#); [Makino & Hut 1997](#); [Mamon 1992, 2000](#)), the tidal stripping, heating and harassment of subhalos, satellite galaxies and globular clusters (e.g., [Moore et al. 1996](#); [Gnedin et al. 1999](#); [van den Bosch et al. 2018](#); [Dutta Chowdhury et al. 2020](#)), the heating of discs ([Ostriker et al. 1972](#)), the formation of stellar binaries by two-body tidal capture ([Fabian et al. 1975](#); [Press & Teukolsky 1977](#); [Lee & Ostriker 1986](#)), and the disruption of star clusters and stellar binaries (e.g., [Spitzer 1958](#); [Heggie 1975](#); [Bahcall et al. 1985](#)). Throughout this paper, for brevity we will refer to the constituent particles of the subject as ‘stars’.

A fully general treatment of gravitational encounters is extremely complicated, which is why they are often studied using numerical simulations. However, in the impulsive limit, when the encounter velocity is large compared to the characteristic internal velocities of the subject, the encounter can be treated analytically. In particular, in this case, one can ignore the

* E-mail: uddipan.banik@yale.edu

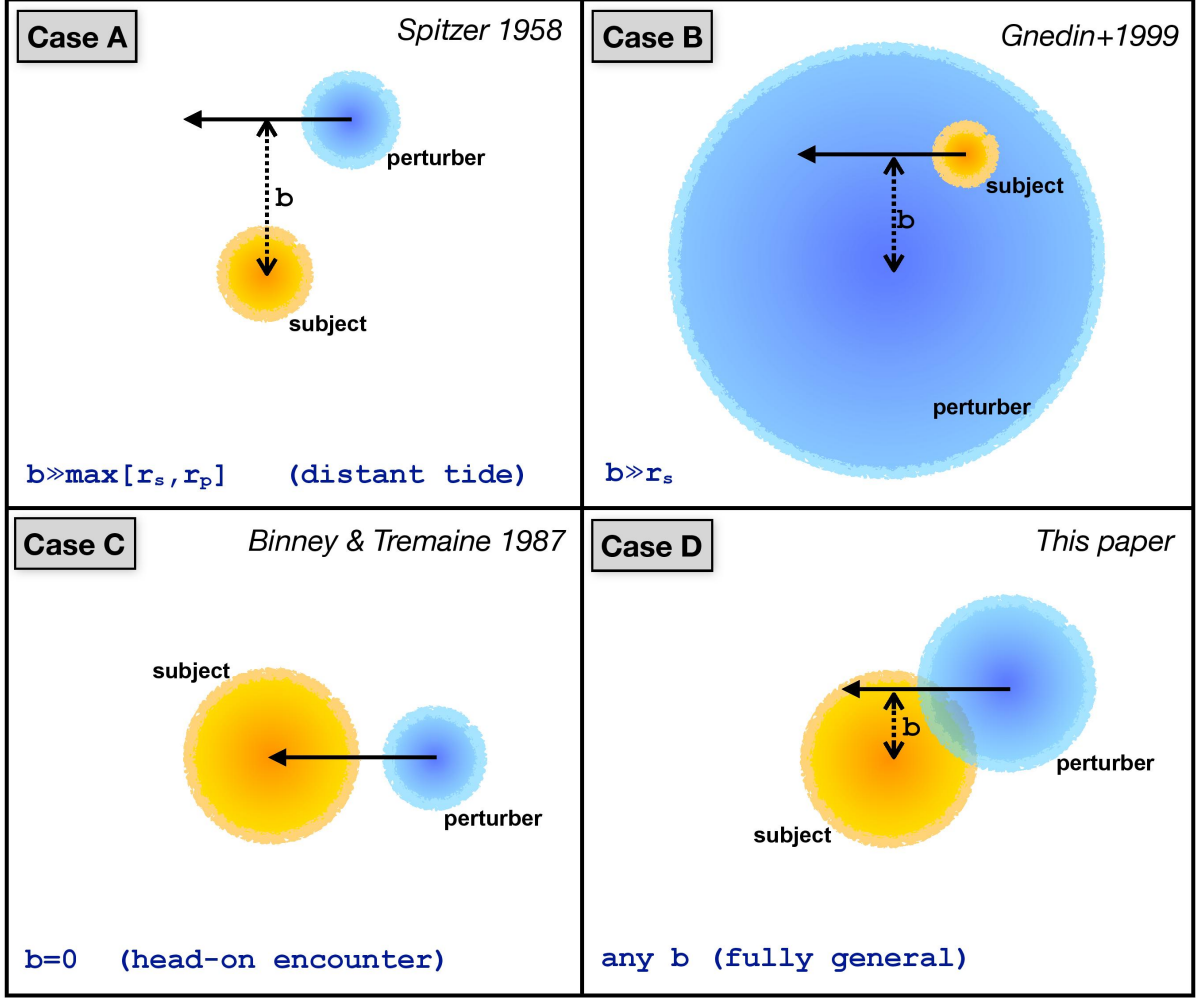


Figure 1: A pictorial comparison of impulsive encounters ($v_P \gg \sigma$) under certain conditions for the impact parameter b . In the upper-right corner of each panel we cite the paper in which the impulsive energy transfer for this case was first worked out. This paper presents the fully general case D (no constraint on b), as depicted in the lower right-hand panel.

internal motion within the subject (i.e., ignore the displacements of the stars during the encounter), and simply compute the velocity change (the impulse) of a star using

$$\Delta \mathbf{v} = - \int \nabla \Phi_P dt, \quad (1)$$

where Φ_P is the potential due to the perturber. And since the encounter speed, v_P , is high, one can further simplify matters by considering the perturber to be on a straight-line orbit with constant speed.

The impulse increases the specific kinetic energy of the subject stars by

$$\Delta \varepsilon = \mathbf{v} \cdot \Delta \mathbf{v} + \frac{1}{2} (\Delta v)^2. \quad (2)$$

Since the potential energy of the stars remains invariant during (but not after) the impulse, the increase in total *internal* energy of the subject is given by

$$\Delta E_{\text{int}} = \int \rho_S(\mathbf{r}) \Delta \varepsilon(\mathbf{r}) d^3 \mathbf{r} - \frac{1}{2} M_S (\Delta v_{\text{CM}})^2. \quad (3)$$

Here M_S and $\rho_S(\mathbf{r})$ are the mass and density profile of the subject and $\Delta \mathbf{v}_{\text{CM}}$ is the velocity impulse of the centre-of-mass of the subject.

If the encounter, in addition to being impulsive, is also distant, such that the impact parameter b is much larger than the scale radii of the subject (r_s) and the perturber (r_P), i.e., $b \gg \max(r_s, r_P)$, then the internal structure of the perturber can be ignored (it can be treated as a point mass), and its potential can be expanded as a multipole series and truncated at the quadrupole term. This ‘distant tide approximation’ (hereafter DTA, depicted as case A in Fig. 1) was first used by [Spitzer \(1958, hereafter S58\)](#) to study the disruption of star clusters by passing interstellar clouds. In particular, Spitzer showed that,

for a spherical subject mass, M_S , an impulsive encounter results in an internal energy increase

$$\Delta E_{\text{int}} = \frac{4M_S}{3} \left(\frac{G M_P}{v_P} \right)^2 \frac{\langle r^2 \rangle}{b^4}, \quad (4)$$

with

$$\langle r^2 \rangle = 4\pi \int \rho_S(r) r^4 dr \quad (5)$$

(see also Table 1). Note that $\Delta E \propto b^{-4}$, indicating that closer encounters are far more efficient in transferring energy than distant encounters. However, as shown by Aguilar & White (1985) using numerical simulations, equation (4) is only accurate for relatively large impact parameters, $b \gtrsim 10 \max(r_S, r_P)$, for which ΔE_{int} is typically extremely small (and thus less interesting).

This situation was improved upon by Gnedin et al. (1999, hereafter GHO99), who modified the treatment by S58 so that it can also be used in cases where $r_S \ll b < r_P$ (see case B in Fig. 1). This describes circumstances in which the subject is moving inside the perturber potential (i.e., a globular cluster moving inside a galaxy, or a satellite galaxy orbiting the halo of the Milky Way). As shown by GHO99, the resulting ΔE_{int} in this case is identical to that of equation (4) but multiplied by a function $\chi_{\text{st}}(b)$, that depends on the detailed density profile of the perturber (see Table 1).

Although this modification by GHO99 significantly extends the range of applicability of the impulse approximation, it is still based on the DTA, which requires that $b \gg r_S$. For smaller impact parameters, ΔE_{int} computed using the method of GHO99 can significantly overpredict the amount of impulsive heating (see §3.1). There is one special case, though, for which ΔE_{int} can be computed analytically, which is that of a head-on encounter ($b = 0$; see Case C in Fig. 1) when both the perturber and the subject are spherical. In that case, as shown in Binney & Tremaine (1987), the symmetry of the problem allows a simple analytical calculation of ΔE_{int} (see Table 1). This was used by van den Bosch et al. (2018) to argue that one may approximate $\Delta E_{\text{int}}(b)$ for *any* impact parameter, b , by simply setting $\Delta E_{\text{int}}(b) = \min[\Delta E_{\text{dt}}(b), \Delta E_0]$. Here $\Delta E_{\text{dt}}(b)$ is the $\Delta E_{\text{int}}(b)$ computed using the DTA of GHO99 (case B in Table 1), and ΔE_0 is the ΔE_{int} for a head-on encounter (case C in Table 1). Although a reasonable assumption, this approach is least accurate exactly for those impact parameters ($b \sim r_S$) that statistically are expected to be most relevant¹.

Another shortcoming of using the DTA is that ΔE_{int} is found to be proportional to $\langle r^2 \rangle$, the mean squared radius of the subject (see equation [5] and Table 1). For most density profiles typically used to model galaxies, dark matter halos, or star clusters, $\langle r^2 \rangle$ diverges, unless the asymptotic radial fall-off of the density is steeper than r^{-5} , or the subject is physically truncated. Although in reality all subjects are indeed truncated by an external tidal field, it is common practice to truncate the density profile of the subject at some arbitrary radius rather than a physically motivated radius. And since $\langle r^2 \rangle$ depends strongly on the truncation radius adopted (see §3.1), this can introduce large uncertainties in the amount of orbital energy transferred to internal energy during the encounter.

In this paper, we develop a fully general, non-perturbative formalism to compute the internal energy change of a subject due to an impulsive encounter. Unlike in the DTA, we do not expand the perturber potential as a multipole series, which assures that our formalism is valid for any impact parameter. For the impulse approximation to be valid, the encounter time $\tau = b/v_P$ has to be small compared to the typical orbital timescale of the subject stars. However, in the distant tide limit, when b is large, the encounter time will also typically be large, rendering the impulse approximation invalid unless v_P is very large. In other words, although there are cases for which the DTA and the impulse approximation are both valid, often they are mutually exclusive. Our formalism, being applicable to all impact parameters, is not hampered by this shortcoming. Moreover, our expression for the internal energy change does not suffer from the $\langle r^2 \rangle$ divergence issue mentioned above, but instead converges, even for infinitely extended systems. This alleviates the problem of having to truncate the galaxy at an arbitrary radius.

This paper is organized as follows. In §2, we present our general formalism to compute the impulse and the energy transferred in impulsive encounters along straight-line orbits. In §3 we apply our formalism to several specific perturber density profiles. In §4 we further generalize the formalism to encounters along eccentric orbits, incorporating an adiabatic correction (Gnedin & Ostriker 1999) to account for the fact that for some subject stars, those with short dynamical times, the impact of the encounter is adiabatic rather than impulsive. In §5, as an astrophysical application of our formalism, we discuss the mass loss of cold dark matter haloes due to tidal shocks during mutual encounters. Finally we summarise our findings in §6.

2 ENCOUNTERS ALONG STRAIGHT-LINE ORBITS

Consider the gravitational encounter between two self-gravitating bodies, hereafter ‘galaxies’. In this section we assume that the two galaxies are mutually unbound to begin with and approach each other along a hyperbolic orbit with initial, relative

¹ For a uniform background of perturbers, the probability that an encounter has an impact parameter in the range b to $b + db$ is $P(b)db \propto b db$, such that the total ΔE due to many encounters is dominated by those with $b \sim r_S$.

Case (1)	Impact parameter (2)	ΔE_{int} (3)	Source (4)
A	$b \gg \max(r_S, r_P)$	$\frac{4M_S}{3} \left(\frac{GM_P}{v_P} \right)^2 \frac{\langle r^2 \rangle}{b^4},$ $\langle r^2 \rangle = \frac{4\pi}{M_S} \int_0^{r_{\text{trunc}}} dr r^4 \rho_S(r)$	[A]
B	$b \gg r_S$	$\frac{4M_S}{3} \left(\frac{GM_P}{v_P} \right)^2 \langle r^2 \rangle \frac{\chi_{\text{st}}(b)}{b^4},$ $\chi_{\text{st}} = \frac{1}{2} [(3J_0 - J_1 - I_0)^2 + (2I_0 - I_1 - 3J_0 + J_1)^2 + I_0^2],$ $I_k(b) = \int_1^\infty \mu_k(b\zeta) \frac{d\zeta}{\zeta^2(\zeta^2 - 1)^{1/2}},$ $J_k(b) = \int_1^\infty \mu_k(b\zeta) \frac{d\zeta}{\zeta^4(\zeta^2 - 1)^{1/2}} \quad (k = 0, 1),$ $\mu_0(R) = \frac{M_P(R)}{M_P}, \quad \mu_1(R) = \frac{d\mu_0(R)}{d \ln R}$	[B]
C	$b = 0$	$4\pi \left(\frac{GM_P}{v_P} \right)^2 \int_0^{r_{\text{trunc}}} \frac{dR}{R} I_0^2(R) \Sigma_S(R),$ $\Sigma_S(R) = 2 \int_R^{r_{\text{trunc}}} \rho_S(r) \frac{r dr}{\sqrt{r^2 - R^2}}$	[C]
D	Any b	$2 \left(\frac{GM_P}{v_P} \right)^2 \left[\int_0^\infty dr r^2 \rho_S(r) \mathcal{J}(r, b) - \mathcal{V}(b) \right],$ $\mathcal{J}(r, b) = \int_0^\pi d\theta \sin \theta \int_0^{2\pi} d\phi s^2 I^2(s), \quad s^2 = r^2 \sin^2 \theta + b^2 - 2br \sin \theta \sin \phi,$ $\mathcal{V}(b) = \frac{1}{M_S} \left[\int_0^\infty dr r^2 \rho_S(r) \mathcal{J}_{\text{CM}}(r, b) \right]^2,$ $\mathcal{J}_{\text{CM}}(r, b) = \int_0^\pi d\theta \sin \theta \int_0^{2\pi} d\phi I(s) [b - r \sin \theta \sin \phi],$ $I(s) = \int_0^\infty d\zeta \frac{1}{R_P} \frac{d\tilde{\Phi}_P}{dR_P},$ $\tilde{\Phi}_P = \Phi_P / (GM_P), \quad R_P = \sqrt{s^2 + \zeta^2}$	[D]

Table 1: Full set of expressions needed to compute ΔE_{int} (considering an impulsive encounter along a straight-line orbit) for the four cases depicted in Fig. 1. Column [2] lists the range of impact parameters for which these expressions are accurate, and column [4] lists the relevant reference, where [A],[B],[C] and [D] correspond to [Spitzer \(1958\)](#), [Gnedin et al. \(1999\)](#), [van den Bosch et al. \(2018\)](#), and this paper, respectively.

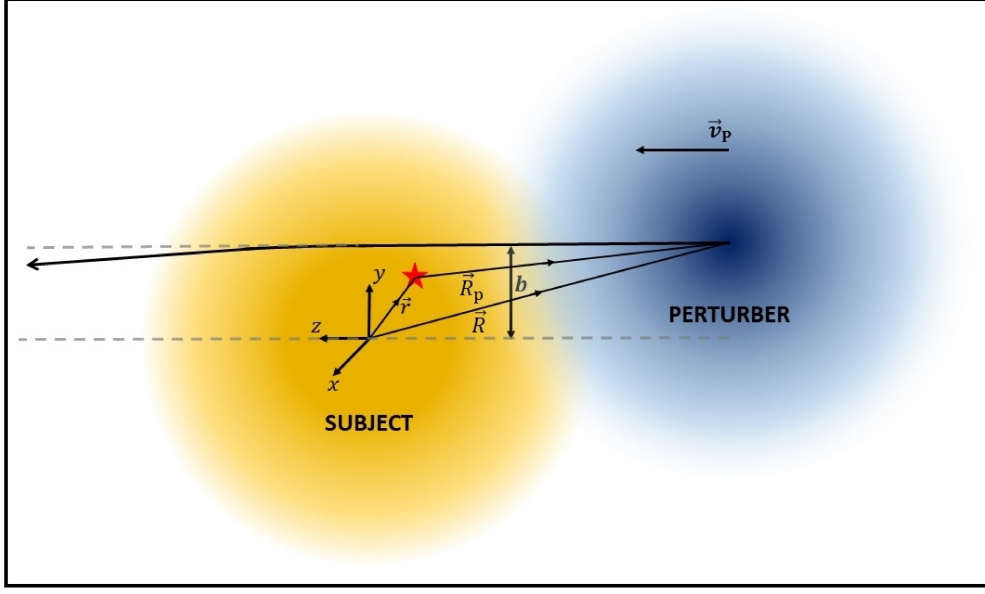


Figure 2: Illustration of the geometry of an impulsive encounter along a nearly straight orbit, specifying the coordinate axes and radial vectors used throughout this paper.

velocity v_P and impact parameter b . For sufficiently fast encounters (large v_P), the deflection of the galaxies from their original orbits due to their mutual gravitational interaction is small and we can approximate the orbits as a straight line. We study the impulsive heating of one of the galaxies (the subject) by the gravitational field of the other (the perturber). Throughout this paper we always assume the perturber to be infinitely extended, while the subject is either truncated or infinitely extended. For simplicity we consider both the perturber and the subject to be spherically symmetric, with density profiles $\rho_P(r)$ and $\rho_S(r)$, respectively. The masses of the subject and the perturber are denoted by M_S and M_P respectively, and r_S and r_P are their scale radii. We take the centre of the unperturbed subject as the origin and define \hat{z} to be oriented along the relative velocity \mathbf{v}_P , and \hat{y} perpendicular to \hat{z} and directed towards the orbit of the perturber. The position vector of a star belonging to the subject is given by \mathbf{r} , that of the COM of the perturber is \mathbf{R} and that of the COM of the perturber with respect to the star is $\mathbf{R}_P = \mathbf{R} - \mathbf{r}$ (see Fig. 2).

2.1 Velocity perturbation up to all orders

During the encounter, the perturber exerts an external, gravitational force on each subject star. The potential due to the perturber flying by with an impact parameter b , on a particle located at $\mathbf{r} = (x, y, z)$ is a function of the distance to the particle from its center, $R_P = |\mathbf{R} - \mathbf{r}| = \sqrt{x^2 + (b - y)^2 + (z - v_P t)^2}$. The acceleration of the star due to the perturbing force is directed along $\hat{\mathbf{R}}_P = \hat{\mathbf{R}} - \hat{\mathbf{r}} = [-x\hat{\mathbf{x}} + (b - y)\hat{\mathbf{y}} - (z - v_P t)\hat{\mathbf{z}}]/R_P$, and is equal to

$$\mathbf{a}_P = -\nabla\Phi_P = \frac{1}{R_P} \frac{d\Phi_P}{dR_P} [-x\hat{\mathbf{x}} + (b - y)\hat{\mathbf{y}} - (z - v_P t)\hat{\mathbf{z}}]. \quad (6)$$

We assume that the perturber moves along a straight-line orbit from $t \rightarrow -\infty$ to $t \rightarrow \infty$. Therefore, under the perturbing force, the particle undergoes a velocity change,

$$\Delta\mathbf{v} = \int_{-\infty}^{\infty} dt \mathbf{a}_P = \int_{-\infty}^{\infty} dt \frac{1}{R_P} \frac{d\Phi_P}{dR_P} [-x\hat{\mathbf{x}} + (b - y)\hat{\mathbf{y}} - (z - v_P t)\hat{\mathbf{z}}]. \quad (7)$$

The integral along $\hat{\mathbf{z}}$ vanishes since the integrand is an odd function of $(z - v_P t)$. Therefore the net velocity change of the particle occurs along the $x - y$ plane and is given by

$$\Delta\mathbf{v} = \frac{2GM_P}{v_P} I(s) [-x\hat{\mathbf{x}} + (b - y)\hat{\mathbf{y}}], \quad (8)$$

where $s^2 = x^2 + (b - y)^2$. The integral $I(s)$ is given by

$$I(s) = \int_0^{\infty} d\zeta \frac{1}{R_P} \frac{d\Phi_P}{dR_P}. \quad (9)$$

Here $\tilde{\Phi}_P = \Phi_P/(GM_P)$, $R_P = \sqrt{s^2 + \zeta^2}$, and $\zeta = v_P t - z$. The integral $I(s)$ contains information about the impact parameter of the encounter as well as the detailed density profile of the perturber. Table. 2 lists analytical expressions for a number of

Perturber profile (1)	$\Phi_P(r)$ (2)	$I(s)$ (3)
Point mass	$-\frac{GM_P}{r}$	$\frac{1}{s^2}$
Plummer sphere	$-\frac{GM_P}{\sqrt{r^2 + r_P^2}}$	$\frac{1}{s^2 + r_P^2}$
Hernquist sphere	$-\frac{GM_P}{r + r_P}$	$\frac{1}{r_P^2 - s^2} \left[1 + \frac{r_P}{\sqrt{r_P^2 - s^2}} \ln \left(\frac{r_P + \sqrt{r_P^2 - s^2}}{s} \right) \right], \quad s < r_P$ $\frac{1}{s^2 - r_P^2} \left[1 - \frac{2r_P}{\sqrt{s^2 - r_P^2}} \tan^{-1} \sqrt{\frac{s - r_P}{s + r_P}} \right], \quad s \geq r_P$
NFW profile	$-\frac{GM_P}{r} \ln \left(1 + \frac{r}{r_P} \right)$	$\frac{1}{s^2} \left[\ln \left(\frac{s}{2r_P} \right) + \frac{r_P}{\sqrt{r_P^2 - s^2}} \ln \left(\frac{r_P + \sqrt{r_P^2 - s^2}}{s} \right) \right], \quad s < r_P$ $\frac{1}{s^2} \left[\ln \left(\frac{s}{2r_P} \right) + \frac{2r_P}{\sqrt{s^2 - r_P^2}} \tan^{-1} \sqrt{\frac{s - r_P}{s + r_P}} \right], \quad s \geq r_P$
Isochrone potential	$-\frac{GM_P}{r_P + \sqrt{r^2 + r_P^2}}$	$\frac{1}{s^2} - \frac{r_P}{s^3} \tan^{-1} \left(\frac{s}{r_P} \right)$
Gaussian potential	$-\frac{GM_P}{r_P} \exp \left[-\frac{r^2}{2r_P^2} \right]$	$\frac{\sqrt{\pi}}{r_P^2} \exp \left[-\frac{s^2}{2r_P^2} \right]$

Table 2: The $I(s)$ integral (see Eq. 9) for different perturber profiles, where $s^2 = x^2 + (b - y)^2$ and $r^2 = s^2 + (z - v_P t)^2$. M_P and r_P are the mass and the scale radius of the perturber respectively. In case of the NFW profile, $M_P = M_{\text{vir}}/f(c)$ where M_{vir} is the virial mass and $f(c) = \ln(1 + c) - c/(1 + c)$, with $c = R_{\text{vir}}/r_P$ the concentration and R_{vir} the virial radius of the NFW perturber.

different perturber potentials, including a point mass, a [Plummer \(1911\)](#) sphere, a [Hernquist \(1990\)](#) sphere, a NFW profile ([Navarro et al. 1997](#)), the Isochrone potential ([Henon 1959](#); [Binney 2014](#)), and a Gaussian potential. The latter is useful since realistic potentials can often be accurately represented using a multi-Gaussian expansion (e.g. [Emsellem et al. 1994](#); [Cappellari 2002](#)).

2.2 Energy dissipation

An impulsive encounter imparts each subject star with an impulse $\Delta \mathbf{v}(\mathbf{r})$. During the encounter, it is assumed that the subject stars remain stagnant, such that their potential energy doesn't change. Hence, the energy change of each star is purely kinetic, and the total change in energy of the subject due to the encounter is given by

$$\Delta E = \int d^3 \mathbf{r} \rho_S(\mathbf{r}) \Delta \varepsilon(\mathbf{r}) = \frac{1}{2} \int d^3 \mathbf{r} \rho_S(r) (\Delta \mathbf{v})^2. \quad (10)$$

Here we have assumed that the unperturbed subject is spherically symmetric, such that its density distribution depends only on $r = |\mathbf{r}|$, and $\Delta\epsilon$ is given by equation (2). We have assumed that the $\mathbf{v} \cdot \Delta\mathbf{v}$ -term (see equation [2]) in $\Delta\epsilon$ vanishes, which is valid for any static, non-rotating, spherically symmetric subject. Plugging in the expression for $\Delta\mathbf{v}$ from equation (8), and substituting $x = r \sin \theta \cos \phi$ and $y = r \sin \theta \sin \phi$, we obtain

$$\Delta E = 2 \left(\frac{GM_P}{v_P} \right)^2 \int_0^\infty dr r^2 \rho_S(r) \mathcal{J}(r, b), \quad (11)$$

where

$$\mathcal{J}(r, b) = \int_0^\pi d\theta \sin \theta \int_0^{2\pi} d\phi s^2 I^2(s), \quad (12)$$

with $s^2 = x^2 + (b - y)^2 = r^2 \sin^2 \theta + b^2 - 2br \sin \theta \sin \phi$.

The above expression of ΔE includes the kinetic energy gained by the COM of the galaxy. From equation (8), we find that the COM gains a velocity

$$\Delta \mathbf{v}_{\text{CM}} = \frac{1}{M_S} \int_0^\infty dr r^2 \rho_S(r) \int_0^\pi d\theta \sin \theta \int_0^{2\pi} d\phi \Delta \mathbf{v} = \frac{2GM_P}{v_P M_S} \int_0^\infty dr r^2 \rho_S(r) \mathcal{J}_{\text{CM}}(r, b) \hat{\mathbf{y}}, \quad (13)$$

where $\mathcal{J}_{\text{CM}}(r, b)$ is given by

$$\mathcal{J}_{\text{CM}}(r, b) = \int_0^\pi d\theta \sin \theta \int_0^{2\pi} d\phi I(s) [b - r \sin \theta \sin \phi]. \quad (14)$$

Note that $\Delta \mathbf{v}_{\text{CM}}$ is not the same as the velocity impulse (equation [8]) evaluated at $\mathbf{r} = (0, 0, 0)$ since we consider perturbations up to all orders. From $\Delta \mathbf{v}_{\text{CM}}$, the kinetic energy gained by the COM can be obtained as follows

$$\Delta E_{\text{CM}} = \frac{1}{2} M_S (\Delta v_{\text{CM}})^2 = 2 \left(\frac{GM_P}{v_P} \right)^2 \mathcal{V}(b), \quad (15)$$

where

$$\mathcal{V}(b) = \frac{1}{M_S} \left[\int_0^\infty dr r^2 \rho_S(r) \mathcal{J}_{\text{CM}}(r, b) \right]^2. \quad (16)$$

We are interested in obtaining the gain in the *internal* energy of the galaxy. Therefore we have to subtract the energy gained by the COM from the total energy gained, which yields the following expression for the internal energy change

$$\Delta E_{\text{int}} = \Delta E - \Delta E_{\text{CM}} = 2 \left(\frac{GM_P}{v_P} \right)^2 \left[\int_0^\infty dr r^2 \rho_S(r) \mathcal{J}(r, b) - \mathcal{V}(b) \right]. \quad (17)$$

As we show in Appendix A, equation (17) has the correct asymptotic behaviour in both the large b and small b limits. For large b it reduces to an expression that is similar to, but also intriguingly different from the standard expression obtained using the DTA, while for $b = 0$ it reduces to the expression for a head-on encounter (case C in Table 1).

3 SPECIAL CASES

In this section we discuss two special cases of perturbers for which the expression for the impulse is analytical, and for which the expression for the internal energy change of the subject can be significantly simplified.

3.1 Plummer perturber

The first special case to be considered is that of a [Plummer \(1911\)](#) sphere perturber, the potential and $I(s)$ of which are given in Table 2. Substituting the latter in equation (12) and analytically computing the ϕ integral yields

$$\mathcal{J}(r, b) = \int_0^\pi d\theta \sin \theta \int_0^{2\pi} d\phi \frac{s^2}{(s^2 + r_P^2)^2} = 4\pi \int_0^1 d\psi \frac{(r^2 - b^2 - r^2 \psi^2) + r_P^2 (r^2 + b^2 - r^2 \psi^2)}{\left[(r^2 - b^2 + r_P^2 - r^2 \psi^2)^2 + 4r_P^2 b^2 \right]^{3/2}}, \quad (18)$$

where $s^2 = r^2 \sin^2 \theta + b^2 - 2br \sin \theta \sin \phi$ and $\psi = \cos \theta$. Similarly substituting the expression for $I(s)$ in equation (14) yields

$$\mathcal{J}_{\text{CM}}(r, b) = \frac{2\pi}{b} \int_0^1 d\psi \left[1 - \frac{r^2 - b^2 + r_P^2 - r^2 \psi^2}{\sqrt{(r^2 - b^2 + r_P^2 - r^2 \psi^2)^2 + 4r_P^2 b^2}} \right], \quad (19)$$

which can be substituted in equation (16) to obtain $\mathcal{V}(b)$. Both these expressions for $\mathcal{J}(r, b)$ and $\mathcal{J}_{\text{CM}}(r, b)$ are easily evaluated using straightforward quadrature techniques. Finally, upon substituting \mathcal{J} and \mathcal{V} in equation (17), we obtain the internal energy change ΔE_{int} of the subject.

Fig. 3 plots the resulting ΔE_{int} , in units of $8\pi(GM_P/v_P)^2 (M_S/r_S^2)$, as a function of the impact parameter, b , for a spherical subject with a [Hernquist \(1990\)](#) density profile. Different panels correspond to different ratios of the characteristic

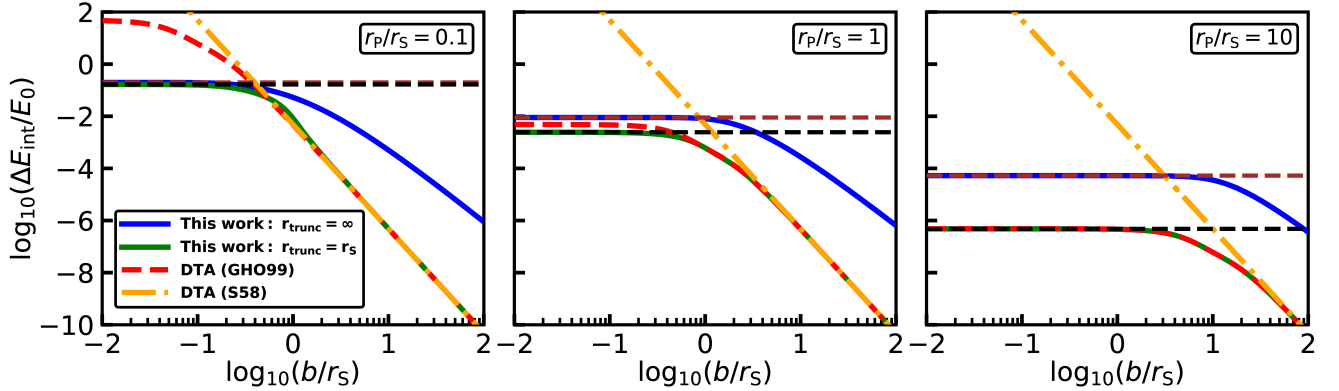


Figure 3: Impulsive heating for encounters along straight-line orbits: Each panel plots ΔE_{int} in units of $E_0 = 8\pi (GM_P/v_P)^2 (M_S/r_S^2)$ as a function of the impact parameter b in units of r_S . Perturber and subject are modelled as Plummer and Hernquist spheres, respectively, with different panels showing results for different ratios of their characteristic radii, as indicated. The solid blue and green lines indicate ΔE_{int} for infinitely extended and truncated ($r_{\text{trunc}} = r_S$) subjects, respectively, computed using our generalized framework (equation [17]). The red, dashed and the orange, dot-dashed lines indicate the ΔE_{int} for the truncated subject obtained using the DTA of GH099 and S58, respectively. The brown and black dashed horizontal lines mark the head-on encounter limits for the infinite and the truncated subjects, respectively. Note that the asymptotic fall-off for the infinitely extended case (solid blue) is shallower than for the truncated case (solid green), which approaches the distant tide limit (dashed red and dot-dashed orange) for large b and saturates to the head-on encounter limit for small b . Also note that the GH099 approximation is in good agreement with the general result as long as the DTA is valid (i.e., b/r_S is large), and/or r_P is significantly larger than r_S .

radii of the perturber, r_P , and the subject, r_S , as indicated. Solid blue lines indicate the ΔE_{int} obtained using our non-perturbative method (equation [17]) for an infinitely extended subject, while the solid green lines show the corresponding results for a subject truncated at r_S . For comparison, the red, dashed and orange, dot-dashed lines show the ΔE_{int} obtained using the DTA of S58 and GH099 (cases A and B in Table 1), respectively, also assuming a Hernquist subject truncated at r_S . Finally, the black and brown horizontal, dashed lines mark the values of ΔE_{int} for a head-on encounter obtained using the expression of van den Bosch et al. (2018) (case C in Table 1) for a truncated and infinitely extended subject, respectively.

Note that ΔE_{int} for the infinitely extended subject has a different asymptotic behaviour for large b than the truncated case. In fact $\Delta E_{\text{int}} \propto b^{-3}$ in the case of an infinitely extended Hernquist subject (when using our non-perturbative formalism), whereas $\Delta E_{\text{int}} \propto b^{-4}$ for a truncated subject (see §A1 for more details).

For large impact parameters, our non-perturbative ΔE_{int} for the truncated case (solid green line) is in excellent agreement with the DTA of S58 and GH099, for all three values of r_P/r_S . In the limit of small b , though, the different treatments yield very different predictions; whereas the ΔE_{int} computed using the method of S58 diverges as b^{-4} , the correction of GH099 causes ΔE_{int} to asymptote to a finite value as $b \rightarrow 0$, but one that is significantly larger than what is predicted for a head-on encounter (at least when $r_P < r_S$). We emphasize, though, that both the S58 and GH099 formalisms are based on the DTA, and therefore not valid in this limit of small b . In contrast, our non-perturbative method is valid for all b , and nicely asymptotes to the value of a head-on encounter in the limit $b \rightarrow 0$.

It is worth pointing out that the GH099 formalism yields results that are in excellent agreement with our fully general, non-perturbative approach when $r_P/r_S \gg 1$, despite the fact that it is based on the DTA. However, this is only the case when the subject is truncated at a sufficiently small radius r_{trunc} . Recall that the DTA yields that $\Delta E_{\text{int}} \propto \langle r^2 \rangle$ (see Table 1), which diverges unless the subject is truncated or the outer density profile of the subject has $d \log \rho_S / d \log r < -5$. In contrast, our generalized formalism yields a finite ΔE_{int} , independent of the density profile of the subject.

This is illustrated in Fig. 4 which plots ΔE_{int} , again in units of $8\pi (GM_P/v_P)^2 (M_S/r_S^2)$, as a function of r_{trunc}/r_S for a Plummer perturber and a truncated Hernquist subject with $r_P/r_S = 1$. Results are shown for three different impact parameters, as indicated. The green and red lines indicate the ΔE_{int} obtained using our general formalism and that of GH099, respectively. Note that the results of GH099 are only in good agreement with our general formalism when the truncation radius is small and/or the impact parameter is large.

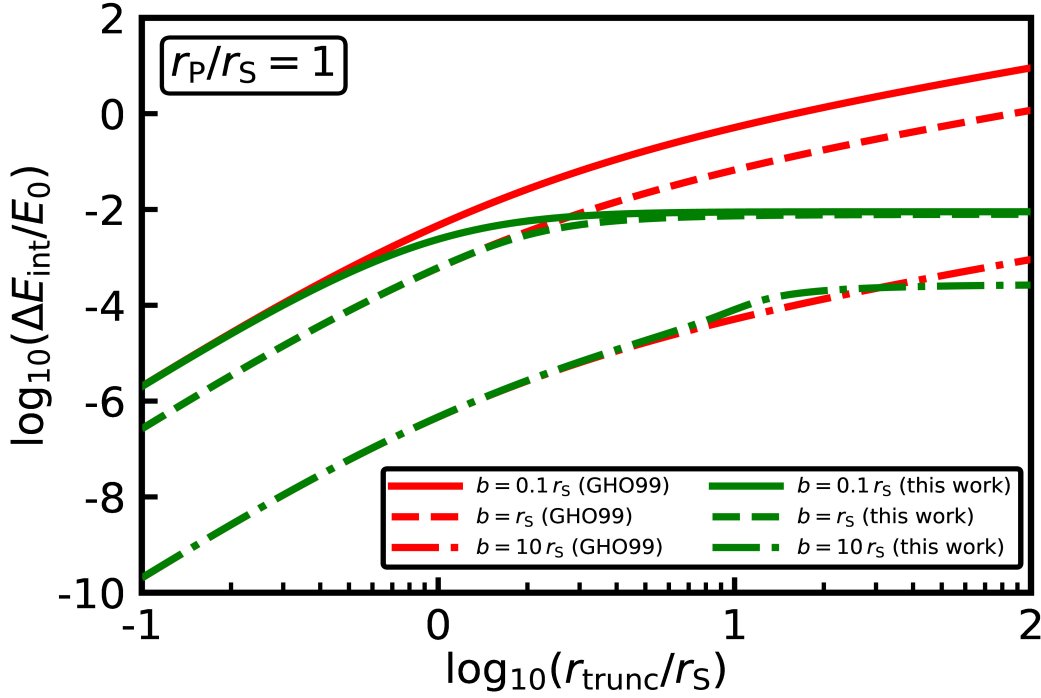


Figure 4: The increase in internal energy, ΔE_{int} , in units of $E_0 = 8\pi(GM_P/v_P)^2 (M_S/r_S^2)$, of a truncated Hernquist sphere due to an impulsive encounter with a Plummer sphere perturber with $r_P/r_S = 1$ along a straight-line orbit. Results are shown as a function of the subject's truncation radius, r_{trunc} , in units of r_S , for three values of the impact parameter, b/r_S , as indicated. Green and red lines correspond to the ΔE_{int} computed using our generalized framework and the DTA of GH099, respectively.

3.2 Point mass perturber

The next special case to discuss is that of a point mass perturber, which one can simply obtain by taking the results for a spherical Plummer perturber discussed above in the limit $r_P \rightarrow 0$. In this limit the \mathcal{J} integral of equation (18) can be computed analytically and substituted in equation (11) to yield

$$\Delta E = 4\pi \left(\frac{GM_P}{v_P} \right)^2 \int_0^\infty dr r^2 \rho_S(r) \int_0^\pi d\theta \frac{\sin \theta}{|b^2 - r^2 \sin^2 \theta|}. \quad (20)$$

The same applies to the \mathcal{J}_{CM} integral of equation (19), which yields the following COM velocity

$$\Delta \mathbf{v}_{\text{CM}} = \frac{2GM_P}{v_P M_S} \frac{M_{\text{enc}}(b)}{b} \hat{\mathbf{y}}, \quad (21)$$

where $M_{\text{enc}}(b)$ is the galaxy mass enclosed within a cylinder of radius b , and is given by

$$M_{\text{enc}}(b) = 4\pi \left[\int_0^b dr r^2 \rho_S(r) + \int_b^\infty dr r^2 \rho_S(r) \left(1 - \sqrt{1 - \frac{b^2}{r^2}} \right) \right]. \quad (22)$$

Therefore, the kinetic energy gained by the COM in the encounter can be written as

$$\Delta E_{\text{CM}} = \frac{1}{2M_S} \left[\frac{2GM_P}{v_P} \frac{M_{\text{enc}}(b)}{b} \right]^2. \quad (23)$$

Subtracting this from the expression for ΔE given in equation (20) and analytically computing the θ integral yields the following expression for the internal energy change

$$\Delta E_{\text{int}} = 8\pi \left(\frac{GM_P}{v_P} \right)^2 \int_0^{r_{\text{trunc}}} dr \rho_S(r) \left[\frac{r}{\sqrt{b^2 - r^2}} \tan^{-1} \left(\frac{r}{\sqrt{b^2 - r^2}} \right) - \frac{r^2}{b^2} \right]. \quad (24)$$

Here we assume the subject to be truncated at some $r_{\text{trunc}} < b$, and therefore $M_{\text{enc}}(b) = M_S$. If $r_{\text{trunc}} > b$, then the point perturber passes through the subject and imparts an infinite impulse in its neighbourhood, which ultimately leads to a divergence of ΔE_{int} .

Note that the term in square brackets tends to $\frac{2}{3}(r/b)^4$ in the limit $r \ll b$. Hence, the above expression for ΔE_{int} reduces to the standard distant tide expression of S58, given in equation (4), as long as $b \gg r_{\text{trunc}}$. Unlike S58 though, the above expression for ΔE_{int} is applicable for any $b > r_{\text{trunc}}$, and is therefore a generalization of the former.

3.3 Other perturbers

The Plummer and point-mass perturbers discussed above are somewhat special in that the corresponding expression for the impulse is sufficiently straightforward that the expression for ΔE_{int} (equation [17]) simplifies considerably. For the other perturber profiles listed in Table 2, ΔE_{int} is to be computed by numerically evaluating the \mathcal{J} and \mathcal{J}_{CM} integrals given in equations (12) and (14), respectively. We provide a Python code, `NP-impulse`², that does so, and that can be used to compute $\Delta E_{\text{int}}(b, v)$ for a variety of (spherical) perturber and subject profiles. We emphasize that the results are in good agreement with the estimates of GHO99, which are based on the DTA, when (i) the perturber is sufficiently extended (i.e., $r_{\text{P}} > r_{\text{S}}$), and (ii) the subject is truncated at a radius $r_{\text{trunc}} < b$. When these conditions are not met, the GHO99 formalism typically significantly overpredicts ΔE_{int} at small impact parameters. Our more general formalism, on the other hand, remains valid for any b and any r_{trunc} (including no truncation), and smoothly asymptotes to the analytical results for a head-on encounter.

4 ENCOUNTERS ALONG ECCENTRIC ORBITS

In the previous sections we have discussed how a subject responds to a perturber that is moving along a straight-line orbit. The assumption of a straight-line orbit is only reasonable in the highly impulsive regime, when $v_{\text{P}} \gg \sigma$. Such situations do occur in astrophysics (i.e., two galaxies having an encounter within a cluster, or a close encounter between two globular clusters in the Milky Way). However, one also encounters cases where the encounter velocity is largely due to the subject and perturber accelerating each other (i.e., the future encounter of the Milky Way and M31), or in which the subject is orbiting within the potential of the perturber (i.e., M32 orbiting M31). In these cases, the assumption of a straight-line orbit is too simplistic. In this section we therefore generalize the straight-line orbit formalism developed in §2, to the case of subjects moving on eccentric orbits within the perturber potential. Our approach is similar to that in GHO99, except that we refrain from using the DTA, i.e., we do not expand the perturber potential in multi-poles and we do not assume that $r_{\text{P}} \gg r_{\text{S}}$. Rather our formalism is applicable to any sizes of the subject and the perturber. In addition, our formalism is valid for any impact parameter (which here corresponds to the pericentric distance of the eccentric orbit), whereas the formalism of GHO99 is formally only valid for $b \gg r_{\text{S}}$. However, like GHO99, our formalism is also based on the impulse approximation, which is only valid as long as the orbit is sufficiently eccentric such that the encounter time, which is of order the timescale of pericentric passage, is shorter than the average orbital timescale of the subject stars. Since the stars towards the central part of the subject orbit much faster than those in the outskirts, the impulse approximation can break down for stars near the centre of the subject, for whom the encounter is adiabatic rather than impulsive. As discussed in §4.3, we can take this ‘adiabatic shielding’ into account using the adiabatic correction formalism introduced by Gnedin & Ostriker (1999). This correction becomes more significant for less eccentric orbits.

4.1 Orbit characterization

We assume that the perturber is much more massive than the subject ($M_{\text{P}} \gg M_{\text{S}}$) and therefore governs the motion of the subject. We also assume that the perturber is spherically symmetric, which implies that the orbital energy and angular momentum of the subject are conserved and that its orbit is restricted to a plane. This orbital energy and angular momentum (per unit mass) are given by

$$\begin{aligned} E &= \frac{1}{2} \dot{R}^2 + \Phi_{\text{P}}(R) + \frac{L^2}{2R^2}, \\ L &= R^2 \dot{\theta}_{\text{P}}, \end{aligned} \tag{25}$$

where \mathbf{R} is the position vector of the COM of the perturber with respect to that of the subject, $R = |\mathbf{R}|$, and θ_{P} is the angle on the orbital plane defined such that $\theta_{\text{P}} = 0$ when R is equal to the pericentric distance, R_{peri} . The dots denote derivatives with respect to time. The above equations can be rearranged and integrated to obtain the following forms for θ_{P} and t as functions of R

$$\begin{aligned} \theta_{\text{P}}(R) &= \int_{1/\alpha}^{R/r_{\text{P}}} \frac{dR'}{R'^2 \sqrt{2[\mathcal{E} - \Phi'_{\text{P}}(R')]/\ell^2 - 1/R'^2}}, \\ t(R) &= \int_{1/\alpha}^{R/r_{\text{P}}} \frac{dR'}{\ell \sqrt{2[\mathcal{E} - \Phi'_{\text{P}}(R')]/\ell^2 - 1/R'^2}}. \end{aligned} \tag{26}$$

Here $\alpha = r_{\text{P}}/R_{\text{peri}}$, t is in units of $(r_{\text{P}}^3/GM_{\text{P}})^{1/2}$, and $\mathcal{E} = E(r_{\text{P}}/GM_{\text{P}})$, $\Phi'_{\text{P}} = \Phi_{\text{P}}(r_{\text{P}}/GM_{\text{P}})$ and $\ell = L/(GM_{\text{P}}r_{\text{P}})^{1/2}$ are dimensionless expressions for the orbital energy, perturber potential and orbital angular momentum, respectively. The resulting orbit is a rosette, with R confined between a pericentric distance, R_{peri} , and an apocentric distance, R_{apo} . The angle

² <https://github.com/uddipanb/NP-impulse>

between a pericenter and the subsequent apocenter is θ_{\max} , which ranges from $\pi/2$ for the harmonic potential to π for the Kepler potential (e.g., Binney & Tremaine 1987). The orbit's eccentricity is defined as

$$e = \frac{R_{\text{apo}} - R_{\text{peri}}}{R_{\text{apo}} + R_{\text{peri}}}, \quad (27)$$

which ranges from 0 for a circular orbit to 1 for a purely radial orbit. Here we follow GH09 and characterize an orbit by e and $\alpha = r_P/R_{\text{peri}}$.

4.2 Velocity perturbation and energy dissipation

The position vector of the perturber with respect to the subject is given by $\mathbf{R} = R \cos \theta_P \hat{\mathbf{y}} + R \sin \theta_P \hat{\mathbf{z}}$, where we take the orbital plane to be spanned by the $\hat{\mathbf{y}}$ and $\hat{\mathbf{z}}$ axes, with $\hat{\mathbf{y}}$ directed towards the pericenter. The function $R(\theta_P)$ specifies the orbit of the subject in the perturber potential and is therefore a function of the orbital parameters α and e . In the same spirit as in equation (6), we write the acceleration due to the perturber on a subject star located at (x, y, z) from its COM as

$$\mathbf{a}_P = -\nabla \Phi_P = \frac{1}{R_P} \frac{d\Phi_P}{dR_P} [-x\hat{\mathbf{x}} + (R \cos \theta_P - y)\hat{\mathbf{y}} + (R \sin \theta_P - z)\hat{\mathbf{z}}], \quad (28)$$

where $R_P = \sqrt{x^2 + (R \cos \theta_P - y)^2 + (R \sin \theta_P - z)^2}$ is the distance of the star from the perturber. We are interested in the response of the subject during the encounter, i.e. as the perturber moves (in the reference frame of the subject) from one apocenter to another, or equivalently from $(R_{\text{apo}}, -\theta_{\max})$ to $(R_{\text{apo}}, \theta_{\max})$. During this period, T , the star particle undergoes a velocity perturbation $\Delta \mathbf{v}$, given by

$$\Delta \mathbf{v} = \int_{-T/2}^{T/2} dt \mathbf{a}_P = \frac{1}{L} \int_{-\theta_{\max}}^{\theta_{\max}} d\theta_P R^2(\theta_P) \frac{1}{R_P} \frac{d\Phi_P}{dR_P} [-x\hat{\mathbf{x}} + (R \cos \theta_P - y)\hat{\mathbf{y}} + (R \sin \theta_P - z)\hat{\mathbf{z}}], \quad (29)$$

where we have substituted θ_P for t by using the fact that $\dot{\theta}_P = L/R^2$. Also, using that $L = \ell\sqrt{GM_P r_P}$ and $\tilde{\Phi}_P = \Phi_P/(GM_P)$, the above expression for $\Delta \mathbf{v}$ can be more concisely written as

$$\Delta \mathbf{v} = \sqrt{\frac{GM_P}{r_P}} \frac{1}{\ell(\alpha, e)} [-xI_1\hat{\mathbf{x}} + (I_2 - yI_1)\hat{\mathbf{y}} + (I_3 - zI_1)\hat{\mathbf{z}}], \quad (30)$$

where

$$\begin{aligned} I_1(\mathbf{r}) &= \int_{-\theta_{\max}}^{\theta_{\max}} d\theta_P R^2(\theta_P) \frac{1}{R_P} \frac{d\tilde{\Phi}_P}{dR_P}, \\ I_2(\mathbf{r}) &= \int_{-\theta_{\max}}^{\theta_{\max}} d\theta_P \cos \theta_P R^3(\theta_P) \frac{1}{R_P} \frac{d\tilde{\Phi}_P}{dR_P}, \\ I_3(\mathbf{r}) &= \int_{-\theta_{\max}}^{\theta_{\max}} d\theta_P \sin \theta_P R^3(\theta_P) \frac{1}{R_P} \frac{d\tilde{\Phi}_P}{dR_P}. \end{aligned} \quad (31)$$

Note that I_1 has units of inverse length, while I_2 and I_3 are unitless.

Over the duration of the encounter, the COM of the subject (in the reference frame of the perturber) undergoes a velocity change

$$\Delta \mathbf{v}_{\text{CM}} = 2 R_{\text{apo}} \dot{\theta}_P|_{\text{apo}} \sin \theta_{\max} \hat{\mathbf{y}} = 2 \sqrt{\frac{GM_P}{r_P}} \alpha \ell(\alpha, e) \frac{1-e}{1+e} \sin \theta_{\max} \hat{\mathbf{y}}. \quad (32)$$

Subtracting this $\Delta \mathbf{v}_{\text{CM}}$ from $\Delta \mathbf{v}$, we obtain the velocity perturbation $\Delta \mathbf{v}_{\text{rel}} = \Delta \mathbf{v} - \Delta \mathbf{v}_{\text{CM}}$ relative to the COM of the subject, which implies a change in internal energy given by

$$\Delta E_{\text{int}} = \frac{1}{2} \int_0^\infty dr r^2 \rho_S(r) \int_0^\pi d\theta \sin \theta \int_0^{2\pi} d\phi \Delta v_{\text{rel}}^2. \quad (33)$$

Substituting the expression for $\Delta \mathbf{v}$ given by equation (30), we have that

$$\Delta E_{\text{int}} = \frac{GM_P}{2r_P} \int_0^\infty dr r^2 \rho_S(r) \int_0^\pi d\theta \sin \theta \int_0^{2\pi} d\phi \mathcal{K}(\mathbf{r}). \quad (34)$$

Here the function $\mathcal{K}(\mathbf{r})$ is given by

$$\mathcal{K}(\mathbf{r}) = \frac{r^2 I_1^2 + I_2'^2 + I_3^2 - 2r I_1 (I_2' \sin \theta \sin \phi + I_3 \cos \theta)}{\ell^2(\alpha, e)}, \quad (35)$$

where $I_2' = I_2 - \Delta \tilde{v}_{\text{CM}}$, with

$$\Delta \tilde{v}_{\text{CM}} = 2\alpha \ell^2(\alpha, e) \frac{1-e}{1+e} \sin \theta_{\max}. \quad (36)$$

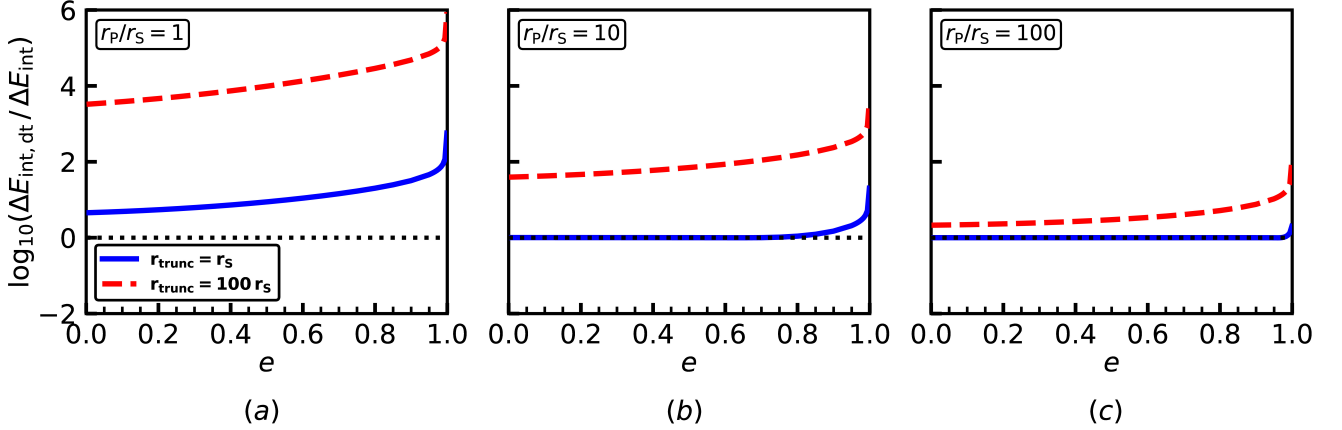


Figure 5: Impulsive heating for encounters along eccentric orbits: Blue, solid and red, dashed lines indicate the ratio of ΔE_{int} computed using the DTA of GH099 ($\Delta E_{\text{int, dt}}$) to that computed using our general formalism (equation [44]) as a function of the orbital eccentricity, e , for cases in which the spherical Hernquist subject is truncated at $r_{\text{trunc}} = r_S$ and $100 r_S$, respectively. In each case, the orbital energy is $E = -0.7GM_P/r_P$, and the perturber is modelled as a Hernquist sphere with $M_P = 1000M_S$ (here M_S is the subject mass enclosed within its truncation radius). Different panels correspond to different r_P/r_S , as indicated.

Finally, from the conservation of energy and equation (25), it is straightforward to infer that³

$$\ell^2(\alpha, e) = \frac{(1+e)^2}{2e} \frac{r_P}{\alpha^2} \left[\tilde{\Phi}_P \left(\frac{r_P}{\alpha} \frac{1+e}{1-e} \right) - \tilde{\Phi}_P \left(\frac{r_P}{\alpha} \right) \right]. \quad (37)$$

4.3 Adiabatic correction

The expression for the internal energy change of the subject derived in the previous section (equation [34]) is based on the impulse approximation. This assumes that during the encounter the stars only respond to the perturbing force and not to the self-gravity of the subject. However, unless the encounter speed is much larger than the internal velocity dispersion of the subject, this is a poor approximation towards the center of the subject, where the dynamical time of the stars, $t_{\text{dyn}}(r) \propto [G\rho_S(r)]^{-1/2}$ can be comparable to, or even shorter than, the time scale of the encounter τ . For such stars the encounter is not impulsive at all; in fact, if $t_{\text{dyn}}(r) \ll \tau$ the stars respond to the encounter adiabatically, such that the net effect of the encounter leaves their energy and angular momentum invariant. In this section we modify the expression for ΔE_{int} derived above by introducing an adiabatic correction to account for the fact that the central region of the subject may be ‘adiabatically shielded’ from the tidal shock.

We follow [Gnedin & Ostriker \(1999\)](#) who, using numerical simulations and motivated by [Weinberg \(1994a,b\)](#), find that the ratio of the actual, average energy change $\langle \Delta E \rangle(r)$ for subject stars at radius r to that predicted by the impulse approximation, is given by

$$\mathcal{A}(r) = [1 + \omega^2(r)\tau^2]^{-\gamma}. \quad (38)$$

Here τ is the shock duration, which is of order the timescale of pericentric passage, i.e.,

$$\tau \sim \frac{1}{\dot{\theta}_P|_{\text{peri}}} = \sqrt{\frac{r_P^3}{GM_P}} \frac{1}{\alpha^2 \ell(\alpha, e)}, \quad (39)$$

and $\omega(r) = \sigma(r)/r$ is the frequency of subject stars at radius r , with $\sigma(r)$ the isotropic velocity dispersion given by

$$\sigma^2(r) = \frac{1}{\rho_S(r)} \int_r^\infty dr' \rho_S(r') \frac{d\Phi_S}{dr'}. \quad (40)$$

For the power-law index γ , [Gnedin & Ostriker \(1999\)](#) find that it obeys

$$\gamma = \begin{cases} 2.5, & \tau \lesssim t_{\text{dyn}} \\ 1.5, & \tau \gtrsim 4 t_{\text{dyn}}, \end{cases} \quad (41)$$

³ Analytical expressions for a few specific perturber potentials are listed in Table 1 of GH099.

where

$$t_{\text{dyn}} = \sqrt{\frac{\pi^2 r_h^3}{2GM_S}} \quad (42)$$

is the dynamical time at the half mass radius r_h of the subject. In what follows we therefore adopt

$$\gamma = 2 - 0.5 \operatorname{erf} \left(\frac{\tau - 2.5 t_{\text{dyn}}}{0.7 t_{\text{dyn}}} \right) \quad (43)$$

as a smooth interpolation between the two limits. Implementing this adiabatic correction, we arrive at the following final expression for the internal energy change of the subject during its encounter with the perturber

$$\Delta E_{\text{int}} = \frac{GM_P}{2r_P} \int_0^\infty dr r^2 \rho_S(r) \mathcal{A}(r) \int_0^\pi d\theta \sin \theta \int_0^{2\pi} d\phi \mathcal{K}(\mathbf{r}). \quad (44)$$

We caution that the adiabatic correction formalism of [Gnedin & Ostriker \(1999\)](#) has not been tested in the regime of small impact parameters. In addition, ongoing studies suggest that equation (38) may require a revision for the case of extensive tides (O. Gnedin, private communication). Hence, until an improved and well-tested formalism for adiabatic shielding is developed, the results in this subsection have to be taken with a grain of salt. However, as long as the adiabatic correction remains a function of radius only, equation (44) remains valid.

In Fig. 5, we compare this ΔE_{int} with that computed using the DTA of GHO99, which can be written in the form of equation (44) but with $\mathcal{K}(\mathbf{r})$ replaced by

$$\mathcal{K}_{\text{GHO}}(\mathbf{r}) = \left(\frac{r}{r_P} \right)^2 \frac{(B_1 - B_3)^2 \sin^2 \theta \sin^2 \phi + (B_2 - B_3)^2 \cos^2 \theta + B_3^2 \sin^2 \theta \cos^2 \phi}{\ell^2(\alpha, e)} \quad (45)$$

with B_1 , B_2 and B_3 integrals, given by equations (36), (37) and (38) in GHO99, that carry information about the perturber profile and the orbit. The lines show the ratio of ΔE_{int} computed using GHO99's DTA and that computed using our formalism (equations [44] and [35]) as a function of the orbital eccentricity e , and for an orbital energy $E = -0.7GM_P/r_P$. Both the perturber and the subject are modelled as Hernquist spheres. Solid blue and dashed red lines correspond to cases in which the subject is truncated at $r_{\text{trunc}} = r_S$ and $100r_S$, respectively, while different panels correspond to different ratios of r_P/r_S , as indicated.

The GHO99 results are in excellent agreement with our more general formalism when $r_{\text{trunc}} = r_S$ and $r_P/r_S \gg 1$. Note, though, that the former starts to overpredict ΔE_{int} in the limit $e \rightarrow 1$. The reason is that for higher eccentricities, the pericentric distance becomes smaller and the higher-order multipoles of the perturber potential start to contribute more. Since the DTA truncates Φ_P at the quadrupole, it becomes less accurate. As a consequence, the GHO99 results actually diverge in the limit $e \rightarrow 1$, while the ΔE_{int} computed using our fully general formalism continues to yield finite values. The agreement between our ΔE_{int} and that computed using the GHO99 formalism becomes worse for smaller r_P/r_S and larger r_{trunc} . When $r_P/r_S = 1$ (left-hand panel), GHO99 overpredicts ΔE_{int} by about one to two orders of magnitude when $r_{\text{trunc}} = r_S$, which increases to 3 to 5 orders of magnitude for $r_{\text{trunc}} = 100r_S$. Once again, this sensitivity to r_{trunc} has its origin in the fact that the integral $\int_0^{r_{\text{trunc}}} dr r^4 \rho_S(r) \mathcal{A}(r)$ diverges as $r_{\text{trunc}} \rightarrow \infty$ for the Hernquist $\rho_S(r)$ considered here.

5 MASS LOSS DUE TO TIDAL SHOCKS IN EQUAL MASS ENCOUNTERS

In this section we present an astrophysical application of our generalized formalism. We consider penetrating gravitational encounters between two cold dark matter haloes. In particular, we examine the amount of mass loss to be expected from such encounters, and, in order to validate our formalism, compare its predictions to the results from N -body simulations.

5.1 Numerical Simulations

We simulate encounters between two identical, spherical NFW halos, whose initial density profiles are given by

$$\rho(r) = \rho_0 \left(\frac{r}{r_s} \right)^{-1} \left(1 + \frac{r}{r_s} \right)^{-2}. \quad (46)$$

Throughout we adopt model units in which the gravitational constant, G , the characteristic scale radius, r_s , and the initial (virial) mass of the halo, M_{vir} , are all unity. Both haloes have an initial concentration parameter $c = r_{\text{vir}}/r_s = 10$, where r_{vir} is the virial radius. We use the method of [Widrow \(2000\)](#) to sample particles from the distribution function (DF) $f = f(E)$ under the assumption that the initial haloes have isotropic velocity distributions, and truncate the haloes at their virial radii. Since the DF that we use to generate the initial conditions is computed using the [Eddington \(1916\)](#) inversion equation, which

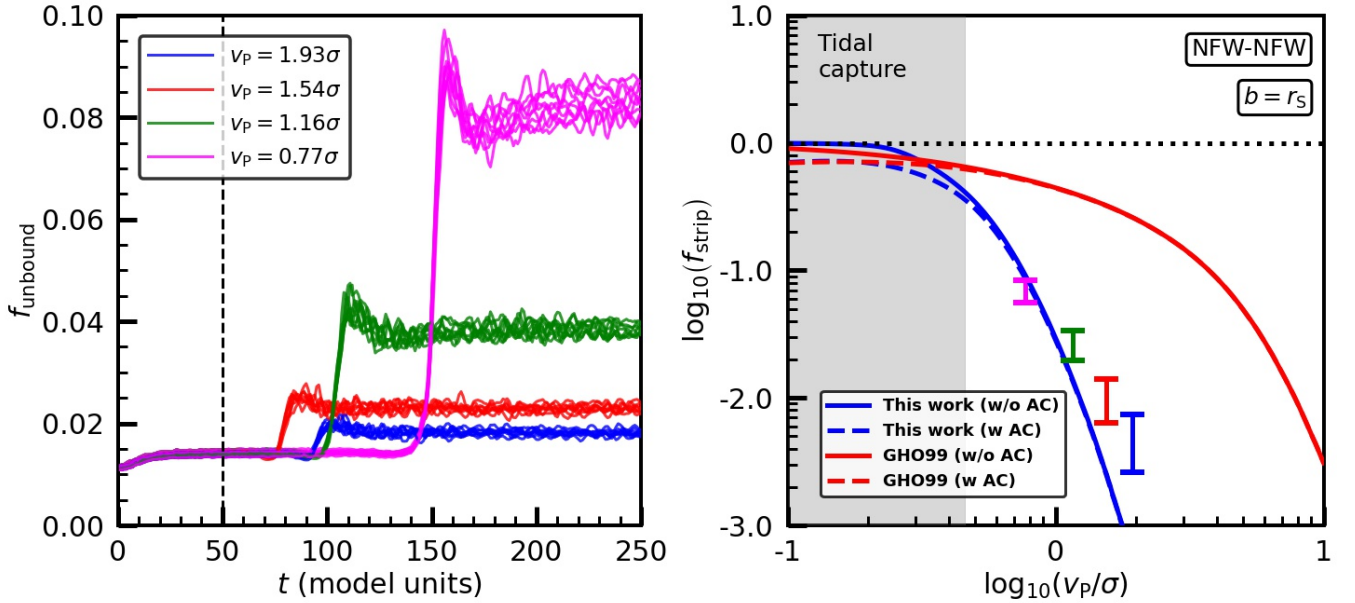


Figure 6: Comparison of numerical simulations with analytical predictions for the amount of mass loss induced by a tidal shock resulting from a penetrating ($b = r_s$) encounter between two identical cold dark matter haloes, modelled as $c = 10$ NFW spheres truncated at the virial radius. Left-hand panel shows the time evolution of the unbound mass fraction, f_{unbound} , of one of the haloes in four series of 10 numerical simulations each with different encounter velocities v_p , as indicated. Right-hand panel shows the comparison with the analytical predictions for the fraction of mass stripped due to the tidal shock, f_{strip} , as a function of v_p/σ (see text for details). Blue and red lines correspond to our general formalism (equation [8]) and the DTA of GHO99, respectively, while solid and dashed lines indicate results obtained with and without adiabatic correction, respectively. Note that the simulation results are in fair agreement with the prediction of our general formalism. We emphasize that GHO99 is not valid for penetrating encounters, and is shown merely for comparison. The grey-shaded region in the right-hand panel indicates the range of v_p/σ for which the encounter results in tidal capture, and eventually a merger of the two haloes, and for which the assumption of a straight-line, impulsive encounter is thus no longer justified.

assumes that the halo extends to infinity, our initial system is not going to be in perfect equilibrium, which has a subtle impact on our results as discussed below⁴. Each halo is modelled using $N_p = 10^5$ particles.

The haloes are initialized to approach each other with an impact parameter $b = r_s$, and an initial velocity v_p . The haloes are initially positioned such that the encounter takes sufficiently long that the haloes have time to virialize in response to the truncation mentioned above (which results in the haloes losing ~ 1.4 percent of their mass to escaping particles). The encounter is followed using the *N*-body code **treecode**, written by Joshua Barnes, which uses a Barnes & Hut (1986) octree to compute accelerations based on a multipole expansion up to quadrupole order, and a second order leap-frog integration scheme to solve the equations of motion. Since we use fixed time step, our integration scheme is fully symplectic. Forces between particles are softened using a simple Plummer softening. Throughout we adopt a time step of $\Delta t = 0.02$ and a softening length of $\varepsilon_{\text{soft}} = 0.05$. As shown in van den Bosch & Ogiya (2018), these values ensure that the halo in isolation remains in equilibrium for at least 10 Gyr. We have run sets of 10 simulations for four different values of v_p/σ each. Here σ is the typical internal velocity dispersion of the NFW halo, given by $\sigma^2 = V_{\text{vir}}^2 g(c)$, with $V_{\text{vir}} = \sqrt{GM_{\text{vir}}/r_{\text{vir}}}$ the virial velocity, and $g(c) = c/[\ln(1+c) - c/(1+c)]$. The 10 simulations for each series are different random realizations of the initial halos, and are used to assess the robustness of the simulations to realization noise, and to put errorbars on the inferred quantities.

We treat one halo as the subject, and measure its fraction of unbound particles, f_{unbound} , as a function of time, using the iterative method described in van den Bosch & Ogiya (2018). The left-hand panel of Fig. 6 shows the time-evolution of f_{unbound} for the 40 different simulations. Different colors correspond to encounters with different v_p/σ , as indicated, while the 10 different curves of the same color show the results from the 10 different random realizations. Note how the subject starts out re-virializing to adjust to the virial truncation, resulting in a loss of ~ 1.4 percent of its mass. Following the

⁴ As an alternative, we could have set up equilibrium haloes using the method described in Kazantzidis et al. (2004), but that results in modified density profiles that are much harder to deal with analytically using our formalism.

encounter, and depending on the encounter speed, the subject loses a substantial amount of mass, after which it revirializes and f_{unbound} undergoes a small oscillation. Since this re-virialization is not accounted for in our generalized formalism, there is some ambiguity in how to compute the mass fraction that becomes unbound. We therefore take a conservative approach and measure for each simulation both the maximum and minimum of f_{unbound} after the epoch of closest approach. We then take the extreme (minimum and maximum) values, f_{extreme} , of f_{unbound} among all 10 simulations in each series, and for both extrema thus obtained we compute $f_{\text{strip}} \equiv (f_{\text{extreme}} - f_0)/(1 - f_0)$ as an indicator of the mass fraction that has been stripped due to the tidal shock. Here $f_0 \equiv f_{\text{unbound}}(t = 50)$, which corrects for the initial re-virialization of the haloes to adjust to the virial truncation. The resulting ranges in f_{strip} are indicated by vertical bars in the right-hand panel of Fig. 6. As expected, encounters of higher velocity result in less mass loss. In fact, although the two haloes penetrate each other, with a distance at closest approach just short of r_s ⁵, the impulsive encounters unbind less than a few percent of the mass. For the smallest encounter velocity considered here, which has $v_p = 0.77\sigma$, the encounter results in the subject losing ~ 6.5 percent of its mass. Using a set of simulations with even lower encounter velocities (not shown) we find that for $v_p/\sigma \lesssim 0.46$ the two haloes actually become bound, resulting in tidal capture and ultimately a merger. Hence, we can conclude that hyperbolic encounters among two NFW haloes only have a modest impact, rarely causing more than a few percent mass loss, even when the encounter is penetrating.

5.2 Comparison with predictions from our formalism

We now turn to our generalized formalism in order to predict f_{strip} for the four different encounters simulated above. We assume that the two haloes encounter each other along a straight-line orbit with an impact parameter $b = r_s$ and (constant) relative velocity v_p . We thus ignore the gravitational focusing that causes the trajectory to deviate slightly from a straight line and the haloes to accelerate (decelerate) just prior to (past) closest approach. This implies that we can compute the impulse $\Delta\mathbf{v}(\mathbf{r})$ for each subject star using equation (8) rather than the more complicated equation (30). In the impulsive limit ($v_p \gg \sigma$), the encounter imparts to a single subject star a specific internal energy given by

$$\Delta\epsilon(\mathbf{r}) = \mathbf{v} \cdot \Delta\mathbf{v}_{\text{rel}} + \frac{1}{2}(\Delta v_{\text{rel}})^2, \quad (47)$$

where $\Delta\mathbf{v}_{\text{rel}}(\mathbf{r}) = \Delta\mathbf{v}(\mathbf{r}) - \Delta\mathbf{v}_{\text{CM}}$. Using our formalism for a straight-line orbit $\Delta\mathbf{v}_{\text{CM}}$ is given by equation (13). For comparison, under the DTA of GH09, $\Delta\mathbf{v}_{\text{rel}}$ is given by equation (10) of their paper. When $v_p \lesssim \sigma$, we have to correct for the adiabatic shielding of the stars towards the central part of the subject. We incorporate this by multiplying $\Delta\epsilon(\mathbf{r})$ of equation (47) by the adiabatic correction factor $\mathcal{A}(r)$, given by equation (38).

We consider a subject star to be stripped if its $\Delta\epsilon/|\epsilon| > 1$, where $\epsilon = v^2/2 + \Phi_S$ is the original binding energy of the star prior to the encounter. To compute the fraction of subject stars that become unbound, f_{strip} , we use the Monte Carlo method of van den Bosch et al. (2018) and sample the isotropic equilibrium distribution function for the spherical $c = 10$ NFW density profile, truncated at its virial radius, with 10^6 particles each. For each particle we compute both $\Delta\epsilon$ and ϵ , and we equate f_{strip} to the fraction of particles for which $\Delta\epsilon > |\epsilon|$. The blue lines in the right-hand panel of Fig. 6 plot the f_{strip} thus obtained as a function of v_p/σ . The dashed and solid lines denote the results obtained with and without adiabatic correction, respectively. Note, though, that this adiabatic correction has almost no impact, except for low encounter velocities that lead to tidal capture, and for which our assumption of a straight-line orbit is clearly not justified.

Overall, the predictions based on our general formalism are in good agreement with the simulation results. There is some indication that the model underpredicts the simulations results for larger v_p/σ . However, this arises as a consequence of the virial truncation used in our simulations: when the simulated halo re-virializes to adjust to this truncation, it not only loses ~ 1.4 of its mass, its outer mass profile is modified from a step-function truncation to a more extended, less steep truncation. Hence, the outskirts of our simulated halos, which are the regions most affected by the tidal shock, are not consistent with the truncated NFW profile adopted in the Monte Carlo sampling of the subject mass. In addition, as mentioned above, our analytical estimation of f_{strip} ignores the gravitational focusing. Despite these shortcomings, we argue that the generalized formalism presented here can be used to make reasonably accurate predictions for the amount of mass stripped off due to a high-speed, penetrating encounter.

For comparison, the red lines in the right-hand panel of Fig. 6 correspond to the f_{strip} predicted using the DTA of GH09. Although the DTA is clearly not valid for penetrating encounters with $b \simeq r_s$, we merely show it here to emphasize that pushing the DTA into a regime where it is not valid can result in large errors. This also highlights the merit of the general formalism presented here, which remains valid in those parts of parameter space where the DTA breaks down.

⁵ Due to gravitational focusing, the distance at closest approach is slightly smaller than the initial impact parameter.

6 CONCLUSIONS

In this paper we have developed a general, non-perturbative formalism to compute the energy transferred due to an impulsive shock. Previous studies (e.g., [Spitzer 1958](#); [Ostriker et al. 1972](#); [Richstone 1975](#); [Aguilar & White 1985](#); [Mamon 1992, 2000](#); [Makino & Hut 1997](#); [Gnedin et al. 1999](#)) have all treated impulsive encounters in the distant tide limit by expanding the perturber potential as a multipole series truncated at the quadrupole term. However, this typically only yields accurate results if the impact parameter, b , is significantly larger than the characteristic sizes of both the subject, r_S , and the perturber, r_P . For such distant encounters, though, very little energy is transferred to the subject and such cases are therefore of limiting astrophysical interest. A noteworthy exception is the case where $r_P \gg r_S$, for which the formalism of [GHO99](#), which also relies on the DTA, yields accurate results even when $b \ll r_P$. However, even in this case, the formalism fails for impact parameters that are comparable to, or smaller than, the size of the subject.

From an astrophysical perspective, the most important impulsive encounters are those for which the increase in internal energy, ΔE_{int} , is of order the subject’s internal binding energy or larger. Such encounters can unbind large amounts of mass from the subject, or even completely destroy it. Unfortunately, this typically requires small impact parameters for which the DTA is no longer valid. In particular, when the perturber is close to the subject, the contribution of higher-order multipole moments of the perturber potential can no longer be neglected. The non-perturbative method presented here overcomes these problems, yielding a method to accurately compute the velocity impulse on a particle due to a high-speed gravitational encounter. It can be used to reliably compute the internal energy change of a subject that is valid for any impact parameter, and any perturber profile. And although the results presented here are, for simplicity, limited to spherically symmetric perturbers, it is quite straightforward to extend it to axisymmetric, spheroidal perturbers, which is something we leave for future work.

In general, our treatment yields results that are in excellent agreement with those obtained using the DTA, but only if (i) the impact parameter b is large compared to the characteristic radii of both the subject and the perturber, and (ii) the subject is truncated at a radius $r_{\text{trunc}} < b$. If these conditions are not met, the DTA typically drastically overpredicts ΔE_{int} , unless one ‘manually’ caps $\Delta E_{\text{int}}(b)$ to be no larger than the value for a head-on encounter, ΔE_0 (see e.g., [van den Bosch et al. 2018](#)). The $\Delta E_{\text{int}}(b)$ computed using our fully general, non-perturbative formalism presented here, on the other hand, naturally asymptotes towards ΔE_0 in the limit $b \rightarrow 0$. Moreover, in the DTA, a radial truncation of the subject is required in order to avoid divergence of the moment of inertia, $\langle r^2 \rangle$. Our method has the additional advantage that it does not suffer from this divergence-problem.

Although our formalism is more general than previous formalisms, it involves a more demanding numerical computation. In order to facilitate the use of our formalism, we have provided a table with the integrals $I(s)$ needed to compute the velocity impulse, $\Delta \mathbf{v}(\mathbf{r})$, given by equation (8), for a variety of perturber profiles (Table 2). In addition, we have released a public Python code, `NP-impulse` (<https://github.com/uddipanb/NP-impulse>) that the reader can use to compute $\Delta \mathbf{v}(\mathbf{r})$ of a subject star as a function of impact parameter, b , and encounter speed, v_P . `NP-impulse` also computes the resulting ΔE_{int} for a variety of spherical subject profiles, and treats both straight-line orbits as well as eccentric orbits within the extended potential of a spherical perturber. In the latter case, `NP-impulse` accounts for adiabatic shielding using the method developed in [Gnedin & Ostriker \(1999\)](#). We hope that this helps to promote the use of our formalism in future treatments of impulsive encounters.

As an example astrophysical application of our formalism, we have studied the mass loss experienced by NFW cold dark matter haloes due to the tidal shocks associated with an impulsive encounter with an identical object along straight-line orbits. In general, our more general formalism agrees well with the results from numerical simulations and predicts that impulsive encounters are less disruptive, i.e., cause less mass loss, than what is predicted based on the DTA of [GHO99](#). Encounters with $v_P/\sigma > 1$ do not cause any significant mass loss ($\lesssim 2\%$). For smaller encounter speeds, mass loss can be appreciable (up to $\sim 10\%$), especially for smaller impact parameters. However, for too low encounter speeds, $v_P/\sigma \lesssim 0.5$, the encounter results in tidal capture, and eventually a merger, something that cannot be treated using the impulse approximation. In addition, for $v_P/\sigma \lesssim 1$, the adiabatic correction starts to become important. Unfortunately, the adiabatic correction of [Gnedin & Ostriker \(1999\)](#) that we have adopted in this paper has only been properly tested for the case of disc shocking, which involves fully compressive tides. It remains to be seen whether it is equally valid for the extensive tides considered here. Ultimately, in this regime a time-dependent perturbation analysis similar to that developed in [Weinberg \(1994b\)](#) may be required to accurately treat the impact of gravitational shocking. Hence, whereas our formalism is fully general in the truly impulsive regime, and for any impact parameter, the case of slow, non-impulsive encounters requires continued, analytical studies.

ACKNOWLEDGEMENTS

The authors are grateful to Oleg Gnedin, Jerry Ostriker and the anonymous referee for insightful comments on an earlier draft of this paper, and to Dhruva Dutta-Chowdhury and Nir Mandelker for valuable discussions. FvdB is supported by the National Aeronautics and Space Administration through Grant Nos. 17-ATP17-0028 and 19-ATP19-0059 issued as part of the Astrophysics Theory Program, and received additional support from the Klaus Tschira foundation.

DATA AVAILABILITY

The data underlying this article, including the Python code `NP-impulse`, is publicly available in the GitHub Repository, at <https://github.com/uddipanb/NP-impulse>.

REFERENCES

- Aguilar L. A., White S. D. M., 1985, *ApJ*, **295**, 374
Bahcall J. N., Hut P., Tremaine S., 1985, *ApJ*, **290**, 15
Barnes J., Hut P., 1986, *Nature*, **324**, 446
Binney J., 2014, arXiv e-prints, p. [arXiv:1411.4937](https://arxiv.org/abs/1411.4937)
Binney J., Tremaine S., 1987, Galactic dynamics. Princeton University Press
Cappellari M., 2002, *MNRAS*, **333**, 400
Dutta Chowdhury D., van den Bosch F. C., van Dokkum P., 2020, arXiv e-prints, p. [arXiv:2008.05490](https://arxiv.org/abs/2008.05490)
Eddington A. S., 1916, *MNRAS*, **76**, 572
Emsellem E., Monnet G., Bacon R., 1994, *A&A*, **285**, 723
Fabian A. C., Pringle J. E., Rees M. J., 1975, *MNRAS*, **172**, 15
Gnedin O. Y., Ostriker J. P., 1999, *ApJ*, **513**, 626
Gnedin O. Y., Hernquist L., Ostriker J. P., 1999, *ApJ*, **514**, 109
Heggie D. C., 1975, *MNRAS*, **173**, 729
Henon M., 1959, *Annales d'Astrophysique*, **22**, 126
Hernquist L., 1990, *ApJ*, **356**, 359
Kazantzidis S., Magorrian J., Moore B., 2004, *ApJ*, **601**, 37
Lee H. M., Ostriker J. P., 1986, *ApJ*, **310**, 176
Makino J., Hut P., 1997, *ApJ*, **481**, 83
Mamon G. A., 1992, *ApJ*, **401**, L3
Mamon G. A., 2000, in Combes F., Mamon G. A., Charmandaris V., eds, *Astronomical Society of the Pacific Conference Series Vol. 197, Dynamics of Galaxies: from the Early Universe to the Present*. p. 377 ([arXiv:astro-ph/9911333](https://arxiv.org/abs/astro-ph/9911333))
Moore B., Katz N., Lake G., Dressler A., Oemler A., 1996, *Nature*, **379**, 613
Navarro J. F., Frenk C. S., White S. D. M., 1997, *ApJ*, **490**, 493
Ostriker J. P., Spitzer Lyman J., Chevalier R. A., 1972, *ApJ*, **176**, L51
Plummer H. C., 1911, *MNRAS*, **71**, 460
Press W. H., Teukolsky S. A., 1977, *ApJ*, **213**, 183
Richstone D. O., 1975, *ApJ*, **200**, 535
Richstone D. O., 1976, *ApJ*, **204**, 642
Spitzer Jr. L., 1958, *ApJ*, **127**, 17
Weinberg M. D., 1994a, *AJ*, **108**, 1398
Weinberg M. D., 1994b, *AJ*, **108**, 1403
White S. D. M., 1978, *MNRAS*, **184**, 185
Widrow L. M., 2000, *ApJS*, **131**, 39
van den Bosch F. C., Ogiya G., 2018, *MNRAS*, **475**, 4066
van den Bosch F. C., Ogiya G., Hahn O., Burkert A., 2018, *MNRAS*, **474**, 3043

APPENDIX A: ASYMPTOTIC BEHAVIOUR

In §2, we obtained the general expression for ΔE_{int} , which is valid for impulsive encounters with any impact parameter b . Here we discuss the asymptotic behaviour of ΔE_{int} in both the distant tide limit (large b) and the head-on limit (small b).

A1 Distant encounter approximation

In the limit of distant encounters, the impact parameter b is much larger than the scale radii of the subject, r_S , and the perturber, r_P . In this limit, it is common to approximate the perturber as a point mass. However, as discussed above, this will yield a diverging ΔE_{int} unless the subject is truncated and $b > r_{\text{trunc}}$ (an assumption that is implied, but rarely mentioned). In order to avoid this issue, we instead consider a (spherical) Plummer perturber. In the limit of large b , equation (17) then reduces to an expression that is similar to, but also intriguingly different from, the standard distant tide expression first obtained by S58 by treating the perturber as a point mass, and expanding Φ_P as a multipole series truncated at the quadrupole term. We also demonstrate that the asymptotic form of ΔE_{int} is quite different for infinite and truncated subjects.

In the large- b limit, we can assume that $r \sin \theta < b$, i.e., we can restrict the domains of the \mathcal{J} and \mathcal{J}_{CM} integrals (equations [18] and [19]) to the inside of a cylinder of radius b . The use of cylindrical coordinates is prompted by the fact that the problem is inherently cylindrical in nature: the impulse received by a subject star is independent of its distance along the direction in which the perturber is moving, but only depends on $R = r \sin \theta$ (cf. equation [7]). Hence, in computing the total energy change, ΔE , it is important to include subject stars with small R but large z -component, while, in the DTA,

those with $R > b$ can be ignored as they receive a negligibly small impulse. Next, we Taylor expand the θ -integrand in the expression for \mathcal{J} about $r \sin \theta = 0$ to obtain the following series expansion for the total energy change

$$\Delta E \approx 4\pi \left(\frac{GM_P}{v_P} \right)^2 \int_0^\infty dr r^2 \rho_S(r) \int_0^\pi d\theta \sin \theta \left[\frac{1}{(1+\varepsilon^2)^2} \frac{1}{b^2} + \frac{1-4\varepsilon^2+\varepsilon^4}{(1+\varepsilon^2)^4} \frac{r^2 \sin^2 \theta}{b^4} + \frac{1-12\varepsilon^2+15\varepsilon^4-2\varepsilon^6}{(1+\varepsilon^2)^6} \frac{r^4 \sin^4 \theta}{b^6} + \dots \right], \quad (\text{A1})$$

where $\varepsilon = r_P/b$. In the large b limit, the COM velocity given by equation (21) reduces to

$$\Delta \mathbf{v}_{\text{CM}} = \frac{2GM_P}{M_S v_P} \frac{\pi}{b} \int_0^\infty dr r^2 \rho_S(r) \int_0^\pi d\theta \sin \theta \left[\frac{2}{1+\varepsilon^2} - \frac{4\varepsilon^2}{(1+\varepsilon^2)^3} \frac{r^2 \sin^2 \theta}{b^2} + \dots \right] \hat{\mathbf{y}}. \quad (\text{A2})$$

The above two integrals have to be evaluated conditional to $r \sin \theta < b$. Upon subtracting the COM energy, $\Delta E_{\text{CM}} = \frac{1}{2} M_S (\Delta v_{\text{CM}})^2$, the first term in the θ integrand of equation (A1) drops out. Integrating the remaining terms yields

$$\Delta E_{\text{int}} \approx 4\pi \left(\frac{GM_P}{v_P} \right)^2 \sum_{n=2}^\infty \mathcal{I}_{n-1} \mathcal{C}_n \left(\frac{r_P}{b} \right) \frac{\mathcal{R}_n(b) + \mathcal{S}_n(b)}{b^{2n}}. \quad (\text{A3})$$

Here

$$\mathcal{C}_n(x) = \frac{P_{2n}(x)}{(1+x^2)^{2n}}, \quad (\text{A4})$$

with $P_{2n}(x)$ a polynomial of degree $2n$. We have worked out the coefficients for $n = 2$ and 3 , yielding $P_4(x) = 1 + x^4$ and $P_6(x) = 1 - 6x^2 + 9x^4 - 2x^6$, and leave the coefficients for the higher-order terms as an exercise for the reader. We do point out, though, that $\mathcal{C}_n(r_P/b) = 1 + \mathcal{O}(r_P^2/b^2)$ in the limit $b \gg r_P$. The coefficient \mathcal{I}_n is given by

$$\mathcal{I}_n = \int_{-1}^1 dx (1-x^2)^n = 2 \sum_{m=0}^n \frac{(-1)^m}{2m+1} \binom{n}{m}, \quad (\text{A5})$$

while $\mathcal{R}_n(b)$ and $\mathcal{S}_n(b)$ are functions of b given by

$$\begin{aligned} \mathcal{R}_n(b) &= \int_0^b dr r^{2n} \rho_S(r), \\ \mathcal{S}_n(b) &= \int_b^\infty dr r^{2n} \rho_S(r) \left[1 - \sqrt{1 - \frac{b^2}{r^2}} \left\{ 1 + \sum_{m=0}^{n-2} \frac{\binom{2m+1}{m}}{2^{2m+1}} \left(\frac{b}{r} \right)^{2m+2} \right\} \right]. \end{aligned} \quad (\text{A6})$$

Note that $\mathcal{R}_n(b)$ is the $(2n-2)^{\text{th}}$ moment of the subject density profile, $\rho_S(r)$, inside a sphere of radius b , while $\mathcal{S}_n(b)$ is the same but for the part of the cylinder outside of the sphere. $\mathcal{R}_n(b) + \mathcal{S}_n(b)$ is therefore the $(2n-2)^{\text{th}}$ moment of $\rho_S(r)$ within the cylinder of radius b . If we truncate the series given in equation (A3) at $n = 2$, then we obtain an asymptotic form for ΔE_{int} that is similar to that of the standard tidal approximation:

$$\Delta E_{\text{int}} \approx \frac{4M_S}{3} \left(\frac{GM_P}{v_P} \right)^2 \frac{\langle r^2 \rangle_{\text{cyl}}}{b^4}. \quad (\text{A7})$$

Here

$$\begin{aligned} \langle r^2 \rangle_{\text{cyl}} &= \frac{4\pi}{M_S} \left[\int_0^b dr r^4 \rho_S(r) + \int_b^\infty dr r^4 \rho_S(r) \left\{ 1 - \sqrt{1 - \frac{b^2}{r^2}} \left(1 + \frac{b^2}{2r^2} \right) \right\} \right] \\ &= \langle r^2 \rangle - \frac{4\pi}{M_S} \int_b^\infty dr r^4 \rho_S(r) \sqrt{1 - \frac{b^2}{r^2}} \left(1 + \frac{b^2}{2r^2} \right). \end{aligned} \quad (\text{A8})$$

which is subtly different from the moment of inertia, $\langle r^2 \rangle$, that appears in the standard expression for the distant tidal limit, and which is given by equation (5). In particular, $\langle r^2 \rangle_{\text{cyl}}$ only integrates the subject mass within a cylinder truncated at the impact parameter, whereas $\langle r^2 \rangle$ integrates over the entire subject mass. As discussed above, this typically results in a divergence, unless the subject is truncated or has a density that falls off faster than r^{-5} in its outskirts.

Indeed, if the subject is truncated at a truncation radius $r_{\text{trunc}} < b$, then $\langle r^2 \rangle_{\text{cyl}} = \langle r^2 \rangle$, and equation (A7) is exactly identical to that for the ‘standard’ impulsive encounter of S58. In addition, $\mathcal{R}_n = \int_0^{r_{\text{trunc}}} dr r^{2n} \rho_S(r)$, which is independent of b , and $\mathcal{S}_n = 0$. Hence, the n^{th} -order term scales as b^{-2n} , and ΔE_{int} is thus dominated by the quadrupole term, justifying the truncation of the series in equation (A1) at $n = 2$.

However, for an infinitely extended subject, or one that is truncated at $r_{\text{trunc}} > b$, truncating the series at the $n = 2$ quadrupole term can, in certain cases, underestimate ΔE_{int} by as much as a factor of ~ 2 . In particular, if $\rho_S(r) \sim r^{-\beta}$ at large r , and falls off less steeply than r^{-5} at small r , then both $\mathcal{R}_n(b)$ and $\mathcal{S}_n(b)$ scale as $b^{2n+1-\beta}$, as long as $\beta < 5$. Hence, all terms in equation (A3) scale with b in the same way, and the truncation is not justified, even in the limit of large impact parameters⁶. Furthermore, in this case it is evident from equation (A3) that $\Delta E_{\text{int}} \sim b^{1-\beta}$. On the other hand, for $\beta = 5$, \mathcal{R}_2

⁶ This is also evident from equation (A1), which shows that all terms contribute equally when $r \sin \theta \sim b$.

is the dominant term and scales with b as $\ln b$, so that $\Delta E_{\text{int}} \sim \ln b/b^4$. For $\beta > 5$, both \mathcal{R}_2 and \mathcal{S}_2 are the dominant terms, which add up to $\langle r^2 \rangle \simeq \int_0^\infty dr r^4 \rho_S(r)$ (which is finite in this case), such that $\Delta E_{\text{int}} \sim b^{-4}$. Hence, for an infinitely extended subject with $\rho_S \propto r^{-\beta}$ at large r we have that

$$\lim_{b \rightarrow \infty} \Delta E_{\text{int}} \propto \begin{cases} b^{1-\beta}, & \beta < 5 \\ b^{-4} \ln b, & \beta = 5 \\ b^{-4}, & \beta > 5. \end{cases} \quad (\text{A9})$$

This scaling is not only valid for an infinitely extended subject, but also for a truncated subject when the impact parameter falls in the range $\max[r_S, r_P] < b < r_{\text{trunc}}$.

A2 Head-on encounter approximation

The head-on encounter corresponds to the case of zero impact parameter (i.e., $b = 0$). As long as the perturber is not a point mass, the internal energy injected into the subject is finite, and can be computed using equation (11) with $b = 0$. Note that there is no need to subtract ΔE_{CM} in this case, since it is zero. If the perturber is a Plummer sphere, the \mathcal{J} integral can be computed analytically for $b = 0$, which yields

$$\Delta E_{\text{int}} = 8\pi \left(\frac{GM_P}{v_P} \right)^2 \int_0^\infty dr \rho_S(r) \mathcal{F}_0(r, r_P), \quad (\text{A10})$$

where

$$\mathcal{F}_0(r, r_P) = \frac{r(2r^2 + r_P^2)}{4(r^2 + r_P^2)^{3/2}} \ln \left[\frac{\sqrt{r^2 + r_P^2} + r}{\sqrt{r^2 + r_P^2} - r} \right] - \frac{r^2}{2(r^2 + r_P^2)}. \quad (\text{A11})$$

It is easily checked that \mathcal{F}_0 has the following asymptotic behaviour in the small- and large- r limits:

$$\mathcal{F}_0(r, r_P) \sim \begin{cases} \frac{2}{3} \left(\frac{r}{r_P} \right)^4, & r \ll r_P \\ \ln \left(\frac{2r}{r_P} \right), & r \gg r_P. \end{cases} \quad (\text{A12})$$

Hence, we see that the behavior of the integrand of equation (A10) in the limits $r \rightarrow 0$ ($r \ll r_P$) and $r \rightarrow \infty$ ($r \gg r_P$), is such that ΔE_{int} is finite, as long as $\rho_S(r)$ scales less steeply than r^{-5} at small r and more steeply than r^{-1} at large r . Both conditions are easily satisfied for any realistic astrophysical subject. Note from equation (A12) that, as expected, more compact perturbers (smaller r_P) dissipate more energy and therefore cause more pronounced heating of the subject.

Note that one obtains the same results using the expression of ΔE_{int} for a head-on encounter listed under case C in Table 1. For a Plummer perturber, $I_0 = R^2/(R^2 + r_P^2)$, which after substitution in the expression for ΔE_{int} , writing $R = r \sin \theta$, and solving the θ -integral, yields equation (A10).

This paper has been typeset from a \LaTeX file prepared by the author.